Escherichia coli Aromatic Amino Acid Aminotransferase: Characterization and Comparison with Aspartate Aminotransferase†

Hideyuki Hayashi,‡ Katsura Inoue,‡ Toshihito Nagata,‡ Seiki Kuramitsu,§ and Hiroyuki Kagamiyama*,‡

Department of Biochemistry, Osaka Medical College, Takatsuki, Osaka 569, Japan, and Department of Biology, Faculty of Science, Osaka University, Toyonaka, Osaka 560, Japan

Received June 15, 1993; Revised Manuscript Received August 12, 1993●

ABSTRACT: Aromatic amino acid aminotransferase (ArAT) from *Escherichia coli* was overexpressed in *E. coli* cells, purified, and characterized. The enzyme was similar to aspartate aminotransferase (AspAT) of *E. coli* in many aspects, such as gross protein structure and spectroscopic properties. The reactions of pyridoxal 5′-phosphate-form ArAT with amino acids and pyridoxamine 5′-phosphate-form ArAT with oxo acids were investigated using stopped-flow spectrophotometric techniques. The kinetic parameters for these "half" reactions could excellently explain the ArAT-catalyzed overall transamination reactions at pH 8.0. Reactions of ArAT with aspartate and tryptophan which had been deuterated at position 2 showed isotope effects of 2.5 and 6.0 in the k_{cat} values of the half-reactions, showing that the proton-transfer step is at least partially rate-limiting for these reactions. ArAT and AspAT showed overlapping substrate specificity. Both ArAT and AspAT were active toward dicarboxylic substrates. ArAT showed, however, 10^3-fold higher activity toward aromatic substrates than AspAT. This high activity toward aromatic substrates was in part ascribed to the active site hydrophobicity of ArAT, which was suggested to be about 1.4 times as large as that of AspAT. In addition to dicarboxylic substrate analogs, aromatic substrate analogs such as carboxylic acids, 2-methyl amino acids, and 3-hydroxy amino acids caused characteristic changes in the absorption spectra of ArAT, while these aromatic analogs did not significantly change the spectra of AspAT. In particular, the *erythro*-3-hydroxy analogs of phenylalanine and aspartate caused a prominent absorption of ArAT at around 500 nm, which is generally ascribed to the accumulation of quinonoid intermediates. The *threo* forms of these 3-hydroxy analogs acted as substrates for ArAT. The *erythro* and *threo* forms of 3-hydroxyaspartate reacted with AspAT similarly as they reacted with ArAT; however, both forms of 3-phenylserine were poor substrates for AspAT, although phenylalanine was a fairly good substrate for AspAT. The observations on the two *erythro*-3-hydroxy amino acids show the similar orientation of these analogs in the active site of ArAT, probably through a hydrogen-bonding network involving the hydroxy groups of the analogs and Tyr70, and suggest that the aromatic binding pocket is near or even overlaps the side-chain-carboxylate-binding site for dicarboxylic substrates.

In *Escherichia coli*, the transamination reaction involving aspartate, tryptophan, phenylalanine, and tyrosine had been known to be catalyzed by "transaminase A" (Rudman & Meister, 1953). Subsequent studies revealed that transaminase A consisted of two enzymes; one is aspartate aminotransferase (AspAT[1]), which is encoded by *aspC* and is not suppressed by tyrosine, and the other is aromatic amino acid aminotransferase (ArAT), which is encoded by *tyrB* and is suppressed by tyrosine (Gelfand & Steinberg, 1977; Gelfand & Rudo, 1977). The primary structure of AspAT has been determined by analysis of the enzyme protein (Kondo et al., 1987) and the *aspC* gene (Kuramitsu et al., 1985b; Malcolm & Kirsch, 1985). The amino acid sequence of ArAT has been deduced from the nucleotide sequence of the *tyrB* gene, the N-terminal amino acid sequence being confirmed by direct analysis of the protein (Kuramitsu et al., 1985a; Fotheringham et al., 1986). The sequence of ArAT showed 43% homology with that of *E. coli* AspAT, and the active site residues of AspAT which had been identified by X-ray crystallography studies (Arnone et al., 1985; Jansonius et al., 1985) were found to be conserved in the primary structure of ArAT at the corresponding position. *E. coli* AspAT has been overproduced in *E. coli* (Kamitori et al., 1987), and analysis of the enzyme showed that AspAT is highly specific to dicarboxylic amino or oxo acids, although it had significant activity toward aromatic amino or oxo acids (Kuramitsu et al., 1990). The catalytic mechanism, as well as the substrate recognition mechanism of AspAT, has long been tested on the basis of several different methodologies including X-ray crystallography and site-directed mutagenesis (Kirsch et al., 1984; Arnone et al., 1985; Jansonius et al., 1985; Hayashi et al., 1990; Fukui et al., 1991; Yano et al., 1993; Toney & Kirsch, 1993; see references therein). On the other hand, the amount of ArAT obtained from *E. coli* is limited and is not adequate for detailed characterization. Preliminary works on isolated ArAT, however, revealed that ArAT, having prominent activity for transaminating aromatic amino and oxo acid substrates, showed activity toward aspartate and oxalacetate comparable to that of AspAT (Powell & Morrison, 1978). Thus ArAT was found to be capable of recognizing two structurally different sets of substrates, the one having an aromatic side chain and the other having an acidic side chain.

† This work was supported by Grant-in-Aids (No. 03780187 and 14454160) from the Ministry of Education, Science, and Culture of Japan.

* Author to whom correspondence should be addressed.

‡ Osaka Medical College.

§ Osaka University.

● Abstract published in *Advance ACS Abstracts,* October 15, 1993.

[1] Abbreviations: ArAT, aromatic amino acid aminotransferase (EC 2.6.1.57); AspAT, aspartate aminotransferase (EC 2.6.1.1); PLP, pyridoxal 5′-phosphate; PMP, pyridoxamine 5′-phosphate; HEPES, *N*-(2-hydroxyethyl)piperazine-*N*′-(2-ethanesulfonic acid); PIPES, piperazine-*N*,*N*′-bis(2-ethanesulfonic acid); CD, circular dichroism; SDS–PAGE, sodium dodecyl sulfate/polyacrylamide gel electrophoresis.

0006-2960/93/0432-12229$04.00/0

In order to understand this characteristic feature of substrate recognition of ArAT, detailed physicochemical analyses of this enzyme are required. Recently we successfully expressed the ArAT protein in *E. coli* by genetic manipulation. This has opened the possibility of gaining further understanding of this enzyme. As a first step in the study of the mechanism of action of ArAT, we purified ArAT expressed in *E. coli* and carried out spectroscopic and kinetic analyses of the enzyme.

MATERIALS AND METHODS

Chemicals. 3-(4-Hydroxyphenyl)propionic acid (fluorometric grade) was obtained from Nacalai Tesque (Kyoto, Japan). 3-Phenylpropionic acid and 3-indolepropionic acid were recrystallized twice from petroleum ether and chloroform, respectively, before use. 3-Indolepyruvic acid, 3-phenylpyruvic acid, 3-(4-hydroxyphenyl)pyruvic acid, DL-*threo*-3-hydroxyaspartic acid, and DL-*threo*-3-phenylserine were obtained from Sigma (St. Louis, MO). L-[2-^{2}H]Aspartate was synthesized as described previously (Kuramitsu et al., 1990). L-[2-^{2}H]Tryptophan was synthesized from L-serine and indole in D_2O using *E. coli* tryptophanase (a generous gift from Dr. Yasushi Kawata, Kyoto University) according to the method of Kiick and Phillips (1988). DL-*erythro*-3-Phenylserine was synthesized by the method of Bergmann et al. (1950). L-*erythro*-3-Hydroxyaspartic acid was synthesized as described by Jenkins (1979). *E. coli* AspAT was prepared as described previously (Kuramitsu et al., 1990). All other chemicals were of the highest grade commercially available.

Expression of the Enzyme. The *Nru*I-*Hin*dIII fragment of the plasmid pMF3 (Kuramitsu et al., 1985a) containing the *tyrB* gene was ligated to the *Hin*cII–*Hin*dIII site of pUC18. The resultant plasmid, named pUC18-*tyrB*, was used to transform *E. coli* TY103, which was derived from JM103 and had a phenotype of *aspC* and *tyrB*, therefore lacking AspAT and ArAT (Yano et al., 1991). The transformed *E. coli* cells were grown in LB media for 10 h, and the cells were harvested in the stationary phase. From a 10-L culture, 40 g of the bacterial cells were collected. The TY103/pUC18-*tyrB* cells expressed about 100 times the ArAT than JM103 cells which had been cultured similarly.

Assay of Enzyme Activity. The ArAT activity was measured according to the method of Inoue et al. (1988). The assay mixture contained in 2 mL, 0.1 M Tris-HCl, pH 8.0, 5 mM L-tryptophan, 20 mM 2-oxoglutarate, 5 μM pyridoxal 5′-phosphate (PLP), and the enzyme. The reaction was started by the addition of enzyme, and the formation of the product 3-indolepyruvate was monitored at 310 nm. The rate of the reaction was calculated using a value of 3180 $M^{-1}\cdot cm^{-1}$ for the difference of the molar absorptivity of 3-indolepyruvate and 2-oxoglutarate at 310 nm (Inoue et al., 1988). One unit of enzyme catalyzes the formation of 1 μmol of 3-indolepyruvate/min at 25 °C.

Purification of the Enzyme. The purification procedure was essentially the same as that of AspAT from *E. coli* JM103 cells harboring the *aspC* overexpression plasmid pKDHE19 (Kamitori et al., 1987), except that tryptophan–2-oxoglutarate transaminating activity was measured to identify the ArAT-containing fractions. About 50 mg of ArAT was usually obtained from 40 g of cells with a yield of 45%. The final preparation showed specific activity of 170 units/mg under the assay conditions.

Preparation of the Pyridoxamine 5′-Phosphate (PMP) Form Enzyme. ArAT is isolated in the PLP form. To obtain the PMP-form enzyme, the PLP-form ArAT was incubated with 50 mM phenylalanine for 10 min at 25 °C in 50 mM HEPES–NaOH buffer, pH 7.0, containing 10 μM PMP. The enzyme was then passed through a PD-10 column (Pharmacia, Uppsala, Sweden) equilibrated with 50 mM HEPES–NaOH buffer, pH 7.0. The eluted enzyme was again incubated with phenylalanine similarly and was gel filtrated to yield the PMP-form ArAT. The PMP-form ArAT thus obtained had the same specific activity as the PLP-form ArAT when they were assayed in the absence of the coenzymes in the assay mixture.

Determination of the Molecular Weight of Native ArAT. A sample of purified ArAT was passed through a Sephacryl S-200 (15 × 600 mm) column equilibrated with 50 mM potassium phosphate buffer, pH 7.0, containing 0.1 M KCl. Standard proteins were chromatographed on the same column similarly. The retention volume of ArAT was compared to those of the other proteins, and M_r for ArAT was calculated. The standard proteins used are bovine thyroglobulin (M_r 670 000), bovine γ-globulin (M_r 158 000), chicken ovalbumin (M_r 44 000), and horse myoglobin (M_r 17 000).

Determination of Kinetic Parameters. The rate of the steady-state transamination reaction with aspartate and 2-oxoglutarate as substrates was measured using malate dehydrogenase (MDH) coupling assay in which the oxidation of NADH by oxalacetate was monitored at 340 nm (Kiick & Cook, 1983). Each 2 mL of reaction mixture contained 50 mM HEPES–NaOH, pH 8.0, 0.1 M KCl, 0.1 mM NADH, 0.025 mg/mL MDH, 0.05–50 mM L-aspartate, and 0.005–20 mM 2-oxoglutarate. The rate of the ArAT-catalyzed steady-state reaction of aromatic amino acids with 2-oxoglutarate was determined by spectrophotometrically measuring the formation of aromatic oxo acids as described previously (Inoue et al., 1988). The reaction conditions are the same as described above for the aspartate–2-oxoglutarate reaction.

Determination of Protein Concentration. The concentration of ArAT subunit in solution was determined spectrophotometrically. The apparent molar extinction coefficients used were $\epsilon_M = 5.3 \times 10^4\ M^{-1}\cdot cm^{-1}$ for the PLP-form enzyme and $\epsilon_M = 5.2 \times 10^4\ M^{-1}\cdot cm^{-1}$ for the PMP-form enzyme at 280 nm. These values were determined based upon the exact protein concentration in the solution determined by the amino acid analysis.

Spectrophotometric Measurements. Absorption spectra were measured using a Hitachi spectrophotometer U-3300. CD spectroscopy was carried out on a JASCO J-500 spectropolarimeter. The buffer solution for the absorption measurements contained 50 mM PIPES–NaOH, 50 mM HEPES–NaOH, or 50 mM sodium borate as buffer component(s), and 0.1 M KCl. The same buffer was used for CD measurements over 250 nm. Protein concentrations were generally $(1–2) \times 10^{-5}$ M. The CD in the range of 200–250 nm was taken in 25 mM potassium phosphate buffer, pH 8.0, containing 0.1 M KCl, with an enzyme concentration of $(1–2) \times 10^{-6}$ M.

Stopped-flow spectrophotometry was performed by Union Giken RA-401. The dead time for this system was 1.5 ms under a pressure of 5.0 $kg\cdot cm^{-2}$.

RESULTS

Structure of ArAT. The purified ArAT showed a single band of M_r 43 000 on SDS–PAGE (data not shown). The size of the subunit agreed well with the value of M_r 43 537 obtained from the amino acid sequence of ArAT which was deduced from the nucleotide sequence of *tyrB* (Kuramitsu et al., 1985a). The N-terminal sequence, analyzed by an Applied

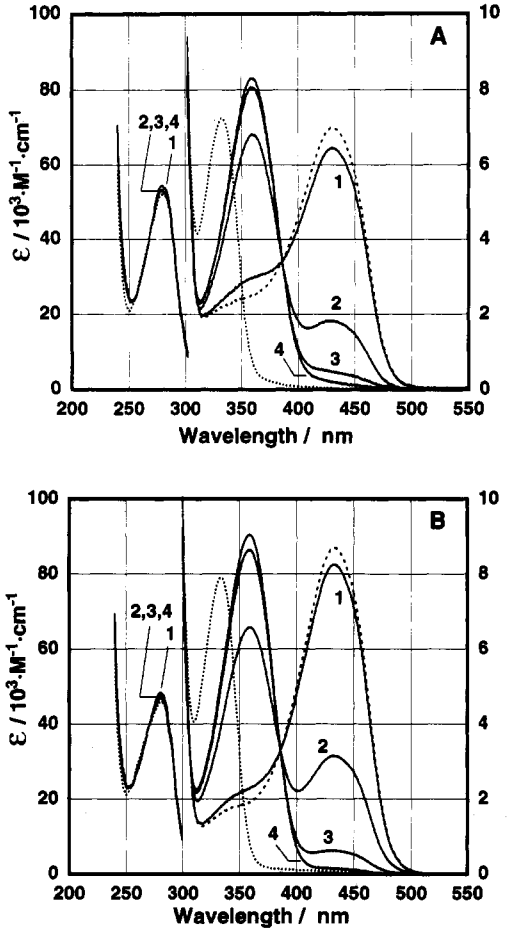

FIGURE 1: Absorption spectra of ArAT (A) and *E. coli* AspAT (B) at 25 °C. In each panel, the solid lines represent the spectra of the PLP-form enzymes at pH 5.6 (curve 1), 7.1 (2), 8.0 (3), and 9.1 (4), and the dotted lines represent those of the PMP-form enzymes at pH 8.0. The spectra were taken in a buffer solution of 50 mM PIPES–NaOH, 50 mM HEPES–NaOH, or 50 mM sodium borate, containing 0.1 M KCl, at an enzyme concentration of 15 μM. The ordinate on the left shows the values for 240–302-nm (ArAT) and 240–300-nm (AspAT) region, and the ordinate on the right side for 302–550-nm (ArAT) and 300–550-nm (AspAT) region. Dashed lines are the estimated absorption spectra of ArAT and AspAT in which the PLP-lysine Schiff bases are in the completely protonated form. The spectra were obtained by calculating the ϵ_{EH} values using the equation: $\epsilon_{EH} = \{(1 + 10^{(pK_a - pH_1)})\epsilon_1 - (1 + 10^{(pK_a - pH_2)})\epsilon_2\}/\{10^{(pK_a - pH_1)} - 10^{(pK_a - pH_2)}\}$, which was derived from eq 1. In this equation, ϵ_1 and ϵ_2 represent the molar absorptivity at pH values of pH_1 and pH_2, respectively.

Biosystems protein sequencer 470A, was Met-Phe-Gln-Lys-Val-Asp-Ala-Tyr-Ala, which was the same as the N-terminal sequence of ArAT purified from *E. coli* W3110 (Kuramitsu et al., 1985a). The molecular weight of the native ArAT was determined to be 83K on Sephacryl S-200 column chromatography (data not shown). Thus, ArAT has a homodimeric structure and in this respect is similar to AspATs from several sources. The purified ArAT contained one PLP per subunit, which was determined by measuring the PLP content in an enzyme solution by the method of Wada and Snell (1961; data not shown).

Absorption Spectrophotometry. The spectra of the PLP-form ArAT at various pH values and the PMP-form ArAT at pH 8.0 are shown in Figure 1A. For comparison, the corresponding spectra of AspAT are shown (Figure 1B). ArAT has 5 tryptophan and 15 tyrosine residues (Kuramitsu et al., 1985a), thereby showing larger molar absorptivity at around 280 nm than AspAT, which has 5 tryptophan and 11 tyrosine residues (Kuramitsu et al., 1985b). There are striking similarities between the spectra of AspAT and ArAT over

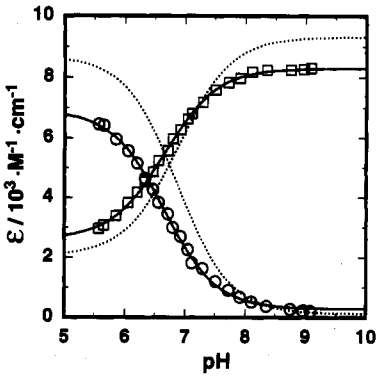

FIGURE 2: The pH dependence of the molar extinction coefficients at 358 (□) and 430 (○) nm for ArAT at 25 °C, in the presence of 50 mM buffer component(s) and 0.1 M KCl. The buffer components are the same as those used in Figure 1. The solid (for ArAT) and dotted (for AspAT) lines represent the theoretical lines drawn by use of eq 1 (see text).

300 nm. Both PMP-form enzymes had absorption maxima at 333 nm. Both PLP-form enzymes showed absorption maxima at 358 nm in the alkaline region and at 430 nm in the acidic region, with an isosbestic point at 385 nm. These pH-dependent spectral changes reflect the ionization of the aldimine nitrogen of the PLP-Lys258[2] Schiff base (Jenkins & Sizer, 1957; Kallen et al., 1985). The molar absorptivity values of ArAT at 358 and 430 nm were plotted against pH and are shown in Figure 2. The pK_a of the aldimine nitrogen of ArAT was obtained to be 6.65 by fitting the plots to the equation

$$\epsilon_{app} = \epsilon_E + \frac{\epsilon_{EH} - \epsilon_E}{1 + 10^{pH - pK_a}} \quad (1)$$

where ϵ_E and ϵ_{EH} denote the molar absorptivity of the basic (E) and acidic (EH) form of the enzyme, respectively. The pH dependency of the molar absorptivity of AspAT at 358 and 430 nm is also shown in Figure 2 (dotted lines). The pK_a of the aldimine nitrogen of AspAT was 6.85, which was 0.2 pH unit higher than that of ArAT. Figure 2 also shows that the molar absorptivity at 430 nm of ArAT was significantly smaller than that of AspAT at low pH. The spectra of ArAT and AspAT in which the aldimine nitrogen is completely protonated were obtained by calculating the ϵ_{EH} values of eq 1 over the wavelength region 300–550 nm and are shown in Figure 1 (dashed lines). The ratio of $\epsilon_{430}/\epsilon_{330}$ was 3.26 for ArAT and 5.65 for AspAT. The absorption around 400–430 nm and that around 330 nm of protonated PLP-lysine Schiff base are generally ascribed to the ketoenamine and enolimine tautomeric forms of the Schiff base, which exist in an equilibrium mixture (Johnson et al., 1970; Hayashi et al., 1993). Therefore, these results show that the Schiff base of ArAT has a greater fraction of enolimine structure than that of AspAT.

CD Spectrophotometry. The CD spectrum of ArAT in the region 200–250 nm was essentially identical to that of AspAT (Yano et al., 1991), suggesting that there was no gross conformational difference between the two enzymes (data not shown). The spectra in the 330–550-nm region of the two enzymes were also very similar (Figure 3). Both spectra showed positive CD at positions corresponding to the absorption bands of the coenzyme and showed similar dependency

[2] The amino acid residue is numbered according to the sequence of pig cytosolic aspartate aminotransferase (Ovchinnikov et al., 1973).

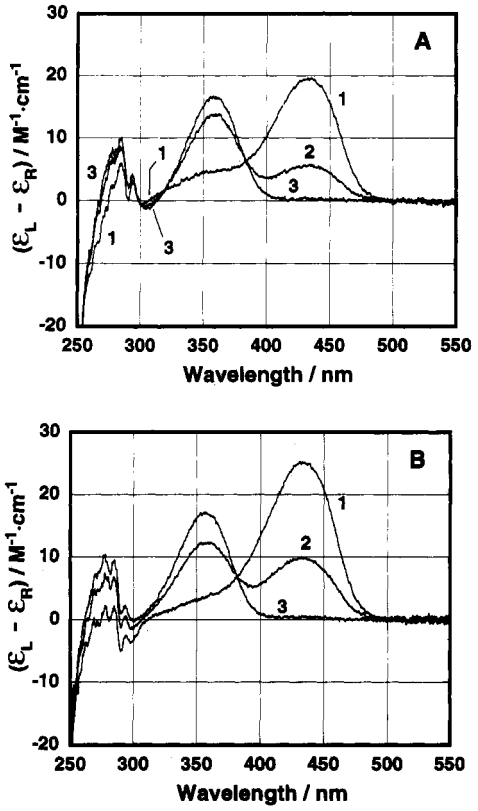

FIGURE 3: CD spectra of ArAT and *E. coli* AspAT in the aromatic and coenzyme region. (A) ArAT and (B) AspAT at pH 5.6 (curve 1), 7.1 (2), and 9.1 (3). The spectra were taken at 25 °C in a buffer solution of 50 mM PIPES–NaOH, 50 mM HEPES–NaOH, or 50 mM sodium borate, containing 0.1 M KCl, at an enzyme concentration of 15 μM, in a 10-mm cell.

on pH. The values of the anisotropic factor $(\epsilon_L - \epsilon_R)/\epsilon$, for ArAT and AspAT at 358 nm were 2.0×10^{-3} and 1.9×10^{-3}, respectively. The values at 430 nm were equally 3.0×10^{-3}. Thus the $(\epsilon_L - \epsilon_R)/\epsilon$ values are almost the same for these two enzymes. This indicates that the effects of the microenvironment around the coenzyme which generates induced optical activity of the bound PLP molecule are essentially identical between the two enzymes. However, there was a striking difference in the pH-dependent change of CD in the aromatic region (250–330 nm). The change of the CD spectra of the two enzymes in the aromatic region occurred concomitantly with the change of those in the coenzyme region. This was manifested in ArAT by the presence of two isosbestic points at 300 and 320 nm. In AspAT, the CD shifted toward negative values with decreasing pH (Figure 3B). In ArAT, the CD below 300 nm also shifted toward negative values, but there was a tendency for the CD between 300 and 320 nm to have more positive values at low pH (Figure 3A). This could result from a difference in the spatial arrangement of the aromatic side chains in relation to the coenzyme Schiff base between the two enzymes. Investigation of which one of the aromatic residues is responsible for this difference in pH-dependent changes in CD is now under way using site-directed mutagenesis.

Reaction of ArAT with Substrates. The reactions of ArAT with dicarboxylic and aromatic amino and oxo acids were studied. On addition of an amino acid substrate to the PLP form of ArAT at pH 8.0, the PLP-form absorption spectrum of the enzyme changed to that of the PMP form, which has a peak at 333 nm (Figure 1). The changes in the absorption spectrum were analyzed similarly as described previously for the reaction of AspAT with substrates (Kuramitsu et al., 1990). In our stopped-flow apparatus with a dead time of 1.5 ms, the reactions were observed to proceed in a monophasic manner. At a fixed substrate concentration the value of the apparent rate constant (k_{app}) was independent of the wavelength used to follow the reaction. The k_{app} values for several different substrate concentrations were obtained by monitoring the reaction at 360 nm. The k_{app} value for glutamate was found to be dependent on the substrate concentration as shown by the following equation:

$$k_{app} = \frac{k_{cat}^{half}[S]}{K_m^{half} + [S]} \quad (2)$$

where K_m^{half} and k_{cat}^{half} are the K_m and k_{cat} values for the "half" reaction, and [S] is the concentration of the amino acid. The k_{app} values for the reactions of ArAT with aspartate, phenylalanine, tyrosine, and tryptophan were significantly affected by the contributions of the reverse reactions of the PMP-form ArAT with corresponding oxo acids. The rates of these reverse reactions were estimated from the K_m^{half} and k_{cat}^{half} values for the oxo acids and were subtracted from the k_{app} values according to the method described for the reaction of AspAT with aspartate (Kuramitsu et al., 1990). The true rate constants for the forward reactions thus calculated showed dependency on substrate concentrations as expressed by eq 2. The K_m^{half} and k_{cat}^{half} values for acidic and aromatic amino acids are summarized in Table I. Several amino acids also showed similar absorption changes; however, saturation of k_{app} with [S] was not apparent, probably owing to high K_m^{half} values relative to the concentrations of the amino acids. In such cases eq 2 was transformed to $k_{app} = (k_{cat}^{half}/K_m^{half})[S]$, and $k_{cat}^{half}/K_m^{half}$ values for these amino acids were obtained and are also shown in Table I.

In the reactions of 3-phenylpyruvate, 3-(4-hydroxyphenyl)-pyruvate, 3-indolepyruvate, oxalacetate, and 2-oxoglutarate with the PMP form of ArAT, the absorption maximum changed from 333 to 358 nm, demonstrating the conversion of the PMP form to the PLP form of the enzyme. The reactions were followed at 360 nm and were analyzed similarly. The K_m^{half} and k_{cat}^{half} values for these oxo acids are shown in Table I.

Table I also shows the rate data for the half-reactions of ArAT with 3-hydroxy amino acids. The details of the reactions are described later.

Equilibrium of the Half-Reaction. The "half"-reaction of the transamination reaction is expressed by the following equation:

$$E_{PLP} + Am \rightleftarrows E_{PMP} + Ox \quad (3)$$

where E_{PLP}, E_{PMP}, Am, and Ox denote the PLP-form enzyme, PMP-form enzyme, an amino acid, and an oxo acid. The equilibrium constant for the half-reaction, K_{eq}^{half}, is defined as

$$K_{eq}^{half} = \frac{[E_{PMP}][Ox]}{[E_{PLP}][Am]} \quad (4)$$

The K_{eq}^{half} values are determined by spectrophotometric titration of the PLP form of ArAT with amino acids (Kuramitsu et al., 1990). The equilibrium constant is related

Table I: Kinetic Parameters of the Reactions of ArAT and AspAT with Amino and Oxo Acids[a]

substrate	ArAT			AspAT[b]		
	k_{cat}^{half} (s^{-1})	K_m^{half} (mM)	$k_{cat}^{half}/K_m^{half}$ ($M^{-1}\cdot s^{-1}$)	k_{cat}^{half} (s^{-1})	K_m^{half} (mM)	$k_{cat}^{half}/K_m^{half}$ ($M^{-1}\cdot s^{-1}$)
phenylalanine	1250	1.0	1250000			200
tyrosine	500	0.83	600000			400
tryptophan	350	0.68	510000	30	34	880
aspartate	290	5.0	58000	550	4.5	120000
glutamate	1200	120	10000	700	38	18000
methionine			920			22
histidine			670			13
leucine			450			2.4
asparagine			18			1.4
glutamine			2.5			0.74
alanine			1.8			0.77
serine			0.098			0.047
threonine			0.074			0.0085
valine			0.17			<0.001
isoleucine			<0.001			<0.001
arginine			0.51			0.0086
lysine			0.48			0.012
3-phenylpyruvate	490	0.025	20000000	56	6.7	8400
3-(4-hydroxyphenyl)pyruvate	650	0.040	16000000	50	3.3	15000
3-indolepyruvate	560	0.057	9800000	54	3.0	18000
oxalacetate	830	0.082	10000000	800	0.035	23000000
2-oxoglutarate	360	1.67	220000	600	1.3	460000
DL-*threo*-3-phenylserine	8.5	8.4[c]	1000[c]			0.0088[c]
DL-*threo*-3-hydroxyaspartate	0.55	16[c]	34[c]	0.93	15[c]	62[c]
DL-*erythro*-3-phenylserine						0.0046[c]

[a] Unless otherwise stated, the substrates are all L-isomers. The reactions were followed by monitoring the change in absorbance at 360 nm in 50 mM HEPES–NaOH buffer containing 0.1 M KCl at 25 °C. The reactions of ArAT with dicarboxylic and aromatic substrates were studied in a stopped-flow spectrophotometer (Union Giken RA-401). Reactions with other amino acids were followed in a standard spectrophotometer. For the reactions which did not show apparent saturation kinetics, only the $k_{cat}^{half}/K_m^{half}$ values are shown. The reactions of *erythro*-3-phenylserine with ArAT and *erythro*-3-hydroxyaspartate with ArAT and AspAT showed complex absorption changes, and the parameters for the half-reactions could not be obtained (see text for detail). [b] Taken from Kuramitsu et al. (1990) except for the data for 3-hydroxy amino acids. [c] Values are for DL-form.

to the kinetic parameters for the half-reaction as follows (see Appendix)

$$K_{eq}^{half} = (k_{cat,Am}^{half}/K_{m,Am}^{half})/(k_{cat,Ox}^{half}/K_{m,Ox}^{half}) \quad (5)$$

where the subscripts Am and Ox denote the value for an amino acid and an oxo acid, respectively. The $1/K_{eq}^{half}$ values for the half-reactions involving aspartate–oxalacetate, glutamate–2-oxoglutarate, phenylalanine–3-phenylpyruvate, tyrosine–3-(4-hydroxyphenyl)pyruvate, and tryptophan–3-indolepyruvate pairs were calculated using eq 5 and the $k_{cat}^{half}/K_m^{half}$ values in Table I to be 170, 22, 16, 27, and 19, respectively. The spectrophotometrically determined $1/K_{eq}^{half}$ values corresponding to those half-reactions are 160, 30, 24, 32, and 19, respectively. The kinetically and spectrophotometrically determined values agree well with each other; therefore, eq 5 is valid for the half-reactions of ArAT with its amino and oxo acid substrates. These results indicate that the observation of the spectral changes upon mixing of ArAT with these amino and oxo acids in this study indeed follows the forward and the reverse reactions of the half-reactions described by eqs 3 and 1a.

Overall Reactions of ArAT. The steady-state transamination reactions catalyzed by ArAT of several pairs of amino acid and oxo acid substrates were analyzed. Double-reciprocal plots of the data fitted well to eq 6, and supported a ping-pong

$$\frac{v}{[E]_T} = \frac{k_{cat}^{overall}}{1 + K_{m,Am}^{overall}/[Am] + K_{m,Ox}^{overall}/[Ox]} \quad (6)$$

Bi Bi mechanism (Velick & Vavra, 1962; Kiick & Cook, 1983). In eq 6, v is the change in product concentration per unit time, and $[E]_T$ is the total enzyme concentration. The values of the parameters $k_{cat}^{overall}$, $K_{m,Am}^{overall}$ and $K_{m,Ox}^{overall}$, are summarized in Table II. These parameters are related to the parameters of the half-reaction by the following equations (Fasella & Hammes, 1967; Kuramitsu et al., 1990; Appendix).

Table II: Kinetic Parameters of the ArAT-Catalyzed Overall-Reactions[a]

substrates	$k_{cat}^{overall}$ (s^{-1})	$K_m^{overall}$ (mM)
phenylalanine	250 (280)	0.26 (0.22)
2-oxoglutarate		1.7 (1.3)
tyrosine	210 (210)	0.32 (0.35)
2-oxoglutarate		1.3 (0.97)
tryptophan	160 (180)	0.50 (0.34)
2-oxoglutarate		0.59 (0.82)
aspartate	140 (160)	3.8 (2.8)
2-oxoglutarate		0.80 (0.75)

[a] The ArAT-catalyzed transamination from aromatic amino acids to 2-oxoglutarate were followed by monitoring the increase in absorption at around 300 nm due to the formation of aromatic oxo acids as described previously (Inoue et al., 1988). Values in parentheses are those calculated using the parameters of the "half"-reactions listed in Table I and eqs 7–9.

$$k_{cat}^{overall} = \frac{k_{Am}^{half} k_{Ox}^{half}}{k_{Am}^{half} + k_{Ox}^{half}} \quad (7)$$

$$K_{m,Am}^{overall} = K_{m,Am}^{half} \frac{k_{Ox}^{half}}{k_{Am}^{half} + k_{Ox}^{half}} \quad (8)$$

$$K_{m,Ox}^{overall} = K_{m,Ox}^{half} \frac{k_{Am}^{half}}{k_{Am}^{half} + k_{Ox}^{half}} \quad (9)$$

Then the values of the overall-reaction parameters were

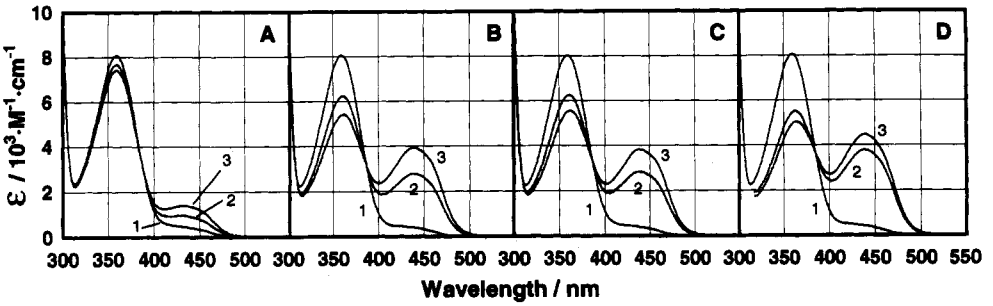

FIGURE 4: Absorption spectra of ArAT in the presence of carboxylic acids. The spectra were taken in 50 mM HEPES–NaOH buffer, pH 8.0, containing 0.1 M KCl, at 25 °C. For all the spectra (A–D), curve 1 represents the spectrum of ArAT: (A) in the presence of 10 mM (curve 2) and 20 mM (curve 3) maleate, (B) 5 mM (curve 2) and 10 mM (curve 3) 3-phenylpropionate, (C) 5 mM (curve 2) and 10 mM (curve 3) 3-(4-hydroxyphenyl)propionate, and (D) 5 mM (curve 2) and 10 mM (curve 3) 3-indolepropionate. In panel D the spectra below 320 nm were omitted due to distortion from the strong absorption of 3-indolepropionate in this wavelength region.

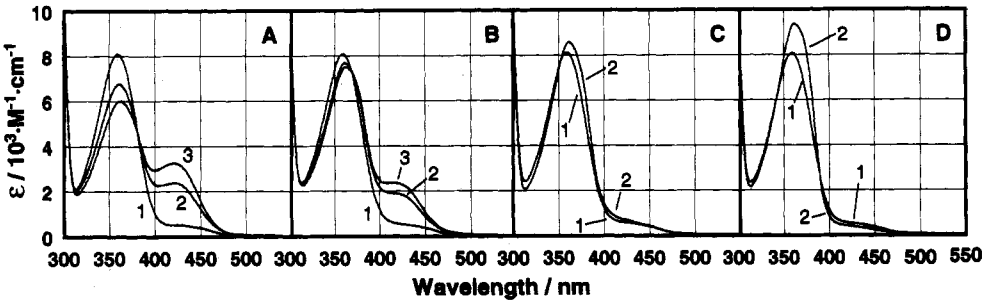

FIGURE 5: Absorption spectra of ArAT in the presence of 2-methyl amino acids. The spectra were taken in 50 mM HEPES–NaOH buffer, pH 8.0, containing 0.1 M KCl, at 25 °C. For all the spectra (A–D), curve 1 represents the spectrum of ArAT: (A) in the presence of 5 mM (curve 2) and 10 mM (curve 3) 2-methyl-DL-aspartate, (B) 5 mM (curve 2) and 10 mM (curve 3) 2-methyl-DL-phenylalanine, (C) 1 mM 2-methyl-L-tyrosine (curve 2), and (D) 10 mM 2-methyl-DL-tryptophan (curve 2). The K_d values are 9.2 mM (DL) for 2-methylaspartate, 5.3 mM (DL) for 2-methylphenylalanine, 1.1 mM (L) for 2-methyltyrosine, and 0.62 mM (DL) for 2-methyltryptophan, at pH 8.0.

calculated using the half-reaction parameters, and the values are listed in Table II in parentheses. The calculated values were found to be in good agreement with the corresponding observed values.

Reactions of ArAT and AspAT with Deuterated Substrates. The primary deuterium isotope effects for removing the proton at position 2 of tryptophan and aspartate were measured. Deuteration at position 2 of both substrates resulted in a significant decrease in the k_{cat}^{half} values. The k_{cat}^{half} value of ArAT for L-[2-^{2}H]tryptophan was 58.5 s^{-1} and that for L-tryptophan was 350 s^{-1}. The k_{cat}^{half} value of AspAT for L-[2-^{2}H]tryptophan was 11.6 s^{-1} and that for L-tryptophan was 30.0 s^{-1}. The k_{cat}^{half} values of ArAT for L-[2-^{2}H]aspartate was 114 s^{-1} and that for L-aspartate was 290 s^{-1}. The K_m^{half} values for these reactions were unchanged. Thus, both ^DV and $^D(V/K)$ values of ArAT are 6.0 for tryptophan and 2.5 for aspartate, and those of AspAT are 2.6 for tryptophan (present work) and 2.2 for aspartate (Kuramitsu et al., 1990).

Reaction of ArAT with Carboxylic Acids. Dicarboxylic acids such as maleate, succinate, and glutarate are competitive inhibitors of AspAT, and they do not form aldimines with PLP when they are bound to the PLP-form AspAT (Jenkins & D'Ari, 1966; Kallen et al., 1985). Hence the complexes are thought to mimic the adsorption complex of AspAT with substrates. The binding of these dianions to the PLP-form AspAT shifts the absorption band at 358 nm to 430 nm due to the increase in the pK_a value of the aldimine formed between PLP and Lys258 by about 2 pH units (Jenkins & D'Ari, 1966). We observed similar absorption changes in ArAT on the binding of dicarboxylic acids. Maleate caused an incrase in absorption at 430 nm and a decrease at 358 nm (Figure 4A). Succinate brought similar absorption changes (data not shown). In addition, we observed that 3-phenylpropionate, 3-(4-hydroxyphenyl)propionate, and 3-indolepropionate, which are structural analogs for phenylalanine, tyrosine, and tryptophan, respectively, bound to ArAT, giving rise to the shift of the absorption band at 358 to 430 nm (Figure 4B–D). These aromatic carboxylic acids did not bring about appreciable changes in the spectra of AspAT (data not shown). The binding of each of the three analogs to ArAT showed a Michaelis–Menten-type dependency on the analog concentration. The K_d values are 8.5 mM for maleate, 6.6 mM for 3-phenylpropionate, 7.0 mM for 3-(4-hydroxyphenyl)propionate, and 3.1 mM for 3-indolepropionate, at pH 8.0. Preliminary works on the pH dependency of the spectra of the ArAT–analog complex showed that the PLP-aldimine pK_a rose by 1.6–2.0 on binding of these analogs.[3]

Reaction of ArAT with 2-Methyl Amino Acids. 2-Methylaspartate binds to the PLP-form AspAT to form an aldimine with PLP but does not undergo further reaction due to the presence of a methyl group at position 2 (Kirsch et al., 1984; Jansonius et al., 1985; Arnone et al., 1985). The spectra of the complexes of pig and *E. coli* AspATs with 2-methylaspartate have two peaks at around 360 and 430 nm and are independent of pH (Fasella et al., 1966; Goldberg et al., 1991; Inoue et al., 1991). Association of 2-methylaspartate with ArAT also gave rise to a similar absorption spectrum with two peaks at 356 and 425 nm (Figure 5A). The reaction of ArAT with 2-methylphenylalanine yielded two peaks at 365 and 430 nm (Figure 5B). Addition of 2-methyltyrosine to ArAT increased the 430-nm band and the absorption band at 358 nm also increased and shifted to 370 nm (Figure 5C). When 2-methyltryptophan was added to ArAT, the absorption at 430 nm was decreased and the absorption band at 358 nm increased and shifted to 370 nm (Figure 5D). These 2-methyl

[3] Hayashi, Kagamiyama, et al., unpublished results.

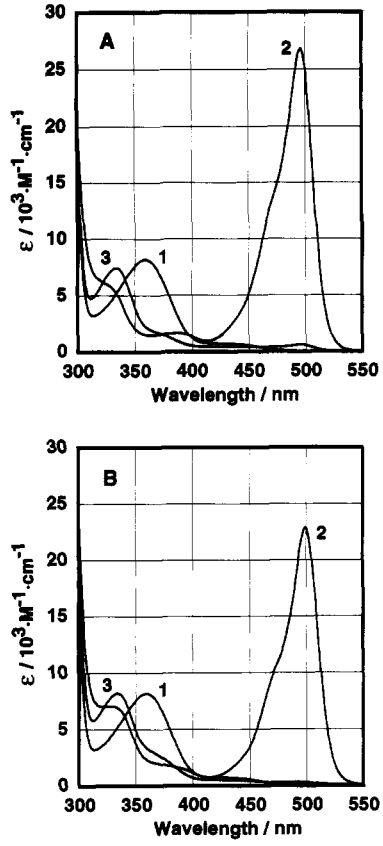

FIGURE 6: Absorption spectra of ArAT in the presence of 3-hydroxy amino acids. The spectra were taken in 50 mM HEPES–NaOH buffer, pH 8.0, containing 0.1 M KCl, at 25 °C. (A) Spectra in the absence (curve 1) and presence of 8.3 mM L-*erythro*-3-hydroxyaspartate (2) and 16.7 mM DL-*threo*-3-hydroxyaspartate (3). (B) Spectra in the absence (1) and presence of 16.7 mM DL-*erythro*-3-phenylserine (2) and 16.7 mM DL-*threo*-3-phenylserine (3).

aromatic amino acids caused no apparent spectral changes when they were reacted with AspAT (data not shown).

Reaction of ArAT and AspAT with 3-Hydroxy Amino Acids. On the reaction of AspAT with *erythro*-3-hydroxyaspartate, the enzyme exhibits an intense absorption around 490 nm that is assigned to the quinonoid intermediate structure of the substrate–coenzyme complex (Jenkins, 1979). We observed a similar absorption spectrum for ArAT–*erythro*-3-hydroxyaspartate complex (Figure 6A, curve 2) with an intense absorption peak at 496 nm. When AspAT and ArAT were reacted with the *threo* form of 3-hydroxyaspartate, the absorption peak of both enzymes shifted from 358 to 330 nm, and only a small absorption peak was observed at around 500 nm (Figure 6A, curve 3; For AspAT, see Jenkins, 1979).

Considering the characteristic reaction of the 3-hydroxy analog of aspartate giving rise to the quinonoid intermediate, it is important to test a similar analog of the aromatic substrate of ArAT, 3-phenylserine, for its reaction with ArAT. The *erythro* form of DL-3-phenylserine indeed reacted with ArAT and gave a 500-nm absorption band with a shoulder at around 470 nm (Figure 6B, curve 2). The shape and intensity of the spectrum were very similar to those of the spectra of the complex of L-*erythro*-3-hydroxyaspartate with AspAT and ArAT (Figure 6A). The spectral changes of the reactions of *erythro*-3-phenylserine and *erythro*-3-hydroxyaspartate with ArAT, when they were followed in a stopped-flow spectrophotometer, proceeded similarly, and were essentially the same as those observed for the reaction of *erythro*-3-hydroxyaspartate with AspAT (Jenkins & Harruff, 1979; data not shown). Briefly, the absorbance at around 500 nm rapidly increased upon mixing ArAT with either of the amino acids and then decreased slowly to the value shown in Figure 6. Virtually none of the PMP-form ArAT seemed to be produced, owing to a high affinity of the product oxo acid for the PMP-form enzyme as suggested by Jenkins and Harruff (1979). Therefore, the k_{cat}^{half} and K_m^{half} values for the half-reactions starting from the PLP-form ArAT and the *erythro*-3-hydroxy amino acids to give the PMP-form ArAT could not be determined experimentally. Some of the rate constants, however, may be obtained by analysis of the spectral transitions described above. Details of the kinetics of these reactions and spectroscopic analysis of the intermediates will be described elsewhere. The reaction of the *threo* form of DL-3-phenylserine with ArAT gave an absorption peak at 330 nm, showing the formation of the PMP-form enzyme, and only a small amount of absorption was observed at around 500 nm (Figure 6B, curve 3). This spectral change was essentially identical to those of the reactions of *threo*-3-hydroxyaspartate with AspAT and ArAT. The kinetic parameters for the half-reactions of *threo*-3-hydroxy amino acids with ArAT are listed in Table I.

The reactions of 3-phenylserine with AspAT were quite different from those with ArAT described above. When either the *erythro* or *threo* form of 3-phenylserine was reacted with AspAT, the absorption of AspAT at 358 nm decreased slowly with a concomitant increase in the absorption at 333 nm, and no detectable absorption was found at around 500 nm. This shows that 3-phenylserine undergoes a very slow transamination with PLP-form AspAT and thus is a slow substrate for AspAT. The $k_{cat}^{half}/K_m^{half}$ values for the reactions of AspAT with *erythro*-3-phenylserine and *threo*-3-phenylserine were 0.0046 $M^{-1}\cdot s^{-1}$ and 0.0088 $M^{-1}\cdot s^{-1}$, respectively (the values are for DL-form). These values were remarkably low compared to the value of 200 $M^{-1}\cdot s^{-1}$ for the reaction of AspAT with phenylalanine (Table I).

DISCUSSION

General Properties of ArAT and Similarity of ArAT to AspAT. Characterization of *E. coli* ArAT demonstrated that the enzyme is in many aspects similar to *E. coli* AspAT. Each enzyme is composed of two identical subunits with M_r of about 43 500 (Kondo et al., 1987; Kuramitsu et al., 1985a). Each enzyme contains one PLP molecule per subunit. The absorption spectra of ArAT and AspAT above 300 nm, which is due to bound PLP, showed a striking resemblance to each other, having two peaks at 358 and at 430 nm (Figure 1). The spectra changed similarly with pH due to the protonation of the PLP-Lys258 aldimine (Kallen et al., 1985). The pK_a values of the aldimine which were determined by pH titration of the spectra both fall in a neutral range, 6.65 for ArAT (Figure 2) and 6.85 for AspAT (Inoue et al., 1991). The CD spectra of ArAT in the protein backbone region (200–250 nm) and those in the coenzyme region (330–550 nm) were essentially the same as those of AspAT (Figure 3). These results suggest that ArAT and AspAT have similar organizations of the whole protein integrity and active-site structure. ArAT reacted with dicarboxylic amino and oxo acids in the same manner as AspAT (Table I). The association of dicarboxylic substrate analogs with ArAT gave complexes which had been observed in AspAT on reaction with these analogs (Figures 4–6). Considering that ArAT and AspAT have 43% sequence homology and the active site residues of AspAT, i.e., Lys258, Tyr70, Trp140, Asn194, Asp222, Tyr225, Arg292, Arg386, are also conserved in the primary structure of ArAT, we think

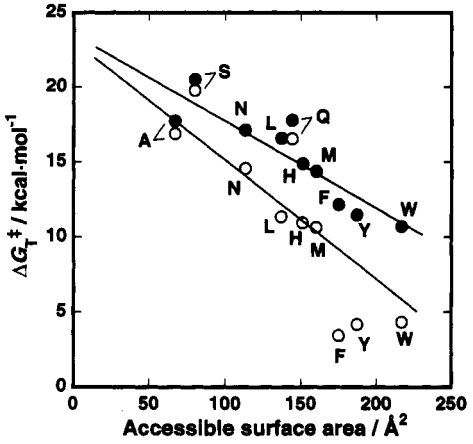

FIGURE 7: $\Delta G_T^{\ddagger}$ values for the reaction of ArAT (○) and *E. coli* AspAT (●) with neutral amino acids was plotted against the accessible surface area (Miller et al., 1987) of the amino acids; pH 8.0, 25 °C. The single letters beside the plots denote amino acids: A, alanine; S, serine; N, asparagine; L, leucine; Q, glutamine; H, histidine; M, methionine; F, phenylalanine; Y, tyrosine; W, tryptophan. The free energy difference ($\Delta G_T^{\ddagger}$) between the transition state (ES‡) and unbound enzyme plus substrate (E+S) was calculated from the $k_{cat}^{half}/K_m^{half}$ value by the equation $\Delta G_T^{\ddagger} = RT(\ln(k_B T/h) - \ln(k_{cat}^{half}/K_m^{half}))$ (Fersht, 1985).

that ArAT has the structural components and functional competence of AspAT which are essential for the catalysis of dicarboxylic substrates.

The most distinguished property of ArAT is its extremely high activity for aromatic amino and oxo acids (Table I). Although *E. coli* AspAT shows significant activity of transaminating aromatic substrates, the activity of ArAT toward aromatic substrates is yet 10^3-fold higher. Thus, ArAT, which seems to have an AspAT-like structural integrity and comparable catalytic efficiency toward dicarboxylic substrates, is at the same time highly adapted to catalyzing transamination of aromatic substrates.

Reaction with Substrates and Substrate Analogs. ArAT can catalyze the transamination of a variety of neutral amino acids besides aromatic amino acids (Table I). In AspAT also, neutral amino acids including aromatic amino acids act as weak substrates, and the reactivity increases with increasing side-chain bulkiness. Plots of the $\Delta G_T^{\ddagger}$ values for the reaction of neutral amino acids with AspAT, which was derived from the $k_{cat}^{half}/K_m^{half}$ values, against the accessible surface area of these neutral amino acids gave a straight line (Kuramitsu et al., 1990). Then, hydrophobic interactions of the amino acid side chain with the active site of *E. coli* AspAT has been suggested, and the strength of the interaction was estimated to be 40 cal·mol^{-1}·Å^{-2} from the slope of the plots. In ArAT, a similar relationship was observed with *nonaromatic* amino acids (Figure 7). The slope of the plots for nonaromatic amino acids was 1.4 times as large as that in the case of AspAT. This and the fact that the enolimine tautomer is relatively more stable in ArAT than in AspAT (Figure 1, dashed lines) may be considered to reflect the relative hydrophobic nature of the active site of ArAT as compared with AspAT. This may assist the binding of aromatic substrates to ArAT. However, the $\Delta G_T^{\ddagger}$ values for aromatic amino acids tended to be considerably lower than those which were estimated by extrapolating the slope of the plots for nonaromatic amino acids to the region for aromatic amino acid substrates. For aromatic amino acid substrates, the $\Delta G_T^{\ddagger}$ values increased with increasing surface area (and the volume) of the substrate side chain. These observations suggest that the mechanism for binding of aromatic amino acids to the active site of ArAT differs from that of nonaromatic amino acids. This will be discussed again later in this section.

It was shown in AspAT that the aminotransferase-catalyzed overall reaction can be treated kinetically as the combination of two half-reactions (Fasella & Hammes, 1967; Kuramitsu et al., 1990). Equations 7–9 describe the relationship between the parameters of the overall-reactions and the half-reactions. In the earlier work on *E. coli* AspAT, it was necessary to assume a "minimum mechanism" in which a half-reaction is composed of three steps: substrate association, intramolecular reaction, and product dissociation process, the intermolecular process being assumed to be rapid (Kuramitsu et al., 1990). As shown in the Appendix, however, without such assumptions eqs 7–9 can apply to any multistep reaction expressed by eq 8a. The experimental validation of eqs 7–9 shows that the assumption of eq 2a is correct and therefore supports the idea that an overall *steady-state* reaction is divided into two parts, either of which can be analyzed kinetically by *single turnover* experiments.

The rates of the half-reactions with dicarboxylic and aromatic substrates were so rapid that only a single relaxation process was observed for each reaction. Therefore, the half-reaction could not be resolved into multiple steps, and the obtained kinetic parameters might contain many microscopic parameters (eq 3a). Further resolution of the half-reaction would require other special kinetic methods such as temperature jump (Fasella & Hammes, 1967) or cryoenzymological technique (Gehring, 1986). Meanwhile, investigations of the reaction process through studying the reaction of ArAT with substrate analogs would provide more information about the reaction mechanism of this enzyme. We therefore investigated spectrophotometrically the reaction of a series of substrate analogs with ArAT. The binding of 3-phenylpropionate, 3-indolepropionate, and maleate to ArAT gave rise to absorption spectra similar to those of the AspAT–maleate complex (Figure 4). These complexes are considered to be the model for adsorption complexes of ArAT with substrates. The increased internal aldimine pK_a values in the complexes suggest that the binding of true substrates to ArAT also increases the internal aldimine pK_a and probably induces the transfer of a proton from the substrate amino group to the aldimine, facilitating the transaldimination reaction. The 2-methyl analogs of dicarboxylic and aromatic amino acids are thought to form "external" aldimines with PLP of ArAT. Both the complexes of ArAT with 2-methylphenylalanine and 2-methylaspartate showed spectra similar to that of the AspAT–2-methylaspartate complex. The spectra, with increased absorption at around 430 nm and a decreased and slightly red-shifted absorption at around 360 nm, have been interpreted to arise from a structure in which a proton is shared between the aldimine and the amino group of Lys258 (Fasella et al., 1966). The reactions of ArAT with 2-methyltyrosine and 2-methyltryptophan were puzzling (Figure 5C,D). The absorption at over 400 nm decreased, and the absorption around 360 nm increased in the presence of 2-methyltryptophan. When 2-methyltyrosine was added to ArAT, the absorption bands at 430 nm and around 360 nm increased. The ratio of the 430-nm absorption to the 360-nm absorption is considered to be determined by the ratio of the probability of the proton residing on the external aldimine to that on Lys258 (Fasella et al., 1966), and the change in the size and shape of the aromatic ring may influence the sharing of the proton by the two basic groups. The spectra of the external aldimines formed between the PLP-form ArAT and true

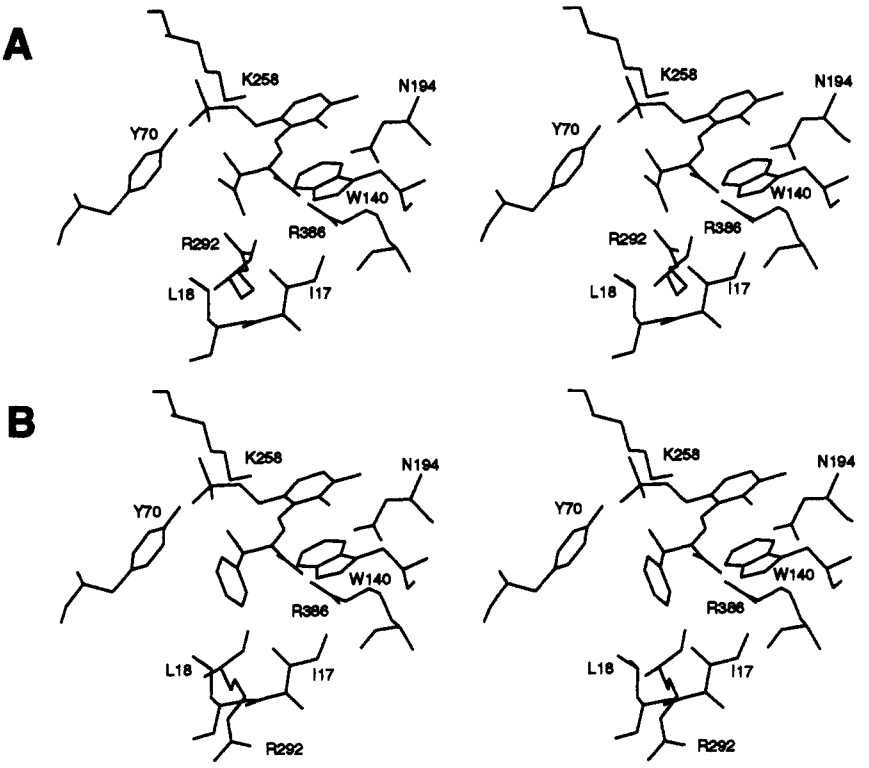

FIGURE 8: Possible structures of the quinonoid intermediates formed between 3-hydroxy amino acids and ArAT as modeled on the structure of *E. coli* AspAT. (A) Complex with *erythro*-3-hydroxyaspartate. *E. coli* AspAT complexed with 2-methylaspartate (Kamitori et al., 1990) was used as the template. 2-Methylaspartate was modified to 3-hydroxyaspartate, and the bond orders of the complex with PLP were adjusted to a quinonoid structure. The atoms of PLP–*erythro*-3-hydroxyaspartate except the phosphate group, and the side chains of Tyr70 and Trp140, were allowed to move, while the positions of all other atoms were fixed. Energy minimization was performed using Insight II/Discover (Biosym Inc.). As the result, the phenol ring of Tyr70 moved 0.8 Å toward Lys258. The ε-amino group of Lys258 was therefore slightly moved manually to avoid contact with Tyr70. The guanidinium group of Arg386 was rotated and torsion angles of the side chain of Arg292 were altered manually so that the two guanidinium groups can approach the carboxylate groups of 3-hydroxyaspartate. (B) Complex with *erythro*-3-phenylserine. Modeling was performed similarly as above except that the position of the side chain of Arg292 was changed to that in the open conformation (Kamitori et al., 1990) in order to accommodate the phenyl ring of *erythro*-3-phenylserine.

substrates are not easily accessible experimentally. However, in the presence of saturating amounts of tryptophan and 3-indolepyruvate, where the external aldimine is supposed to accumulate, the spectra showed a peak at 430 nm rather than at 360 nm, suggesting that the protonated external aldimine is dominant.[4] It may then be considered that the presence of the 2-methyl group may have caused alterations in the external aldimine structure of ArAT with tryptophan and tyrosine.

The 496-nm absorption peak that is produced upon reaction of AspAT with *erythro*-3-hydroxyaspartate has been interpreted as the quinonoid structure of PLP–substrate complex (Jenkins, 1979). The quinonoid structure of the *erythro*-3-hydroxyaspartate–PLP complex is supposed to be stabilized by a pair of strong hydrogen bonds from the phenolic oxygen of Tyr70 to 3-O of *erythro*-3-hydroxyaspartate and to an oxygen atom of the phosphate group (Taylor & Metzler, 1990). This also explains the observation that *threo*-3-hydroxyaspartate is a substrate and does not give a 496-nm absorption (Jenkins, 1979), because the OH group in *threo* configuration cannot form a strong hydrogen bond with Tyr70. Taking this into account, the reaction of 3-phenylserine with ArAT has important implications for the mode of binding of the phenyl ring of phenylalanine to ArAT. The *erythro* form of 3-phenylserine produced an intense 500-nm band, whereas the *threo* form gave a 333-nm band as a result of transamination (Figure 6). These results can be explained clearly by assuming the structures shown in Figure 8. Figure 8 shows proposed structures of the complexes of ArAT with L-*erythro*-3-hydroxyaspartate and L-*erythro*-3-phenylserine modeled as quinonoid intermediates on the structure of *E. coli* AspAT. In these models the 3-O atoms of *erythro*-3-hydroxyaspartate and *erythro*-3-phenylserine form hydrogen bonds with Tyr70, and the configuration of *erythro*-3-phenylserine and *erythro*-3-hydroxyaspartate are superimposable. Therefore, the above observations strongly suggest that in the quinonoid structure, and possibly also in the other intermediate structures, the phenyl ring of phenylalanine is located near the position occupied by the 3-carboxylate group of aspartate during the reaction of aspartate with ArAT. The entire sequence of ArAT has been modeled on the X-ray structure of chicken mitochondrial AspAT (Seville et al., 1988). The phenol ring of the substrate tyrosine modeled as the external aldimine in this hypothetical active site occupies the position between Leu18 and Trp140; this proposal is essentially consistent with our results. The configuration of the substrate aromatic ring in the active site as discussed above would require the side chain of Arg292 to be placed properly to avoid unfavorable contact with the substrate aromatic ring (Figure 8B). Thus the function of the residue Arg292 of ArAT, which is supposed to behave differently toward dicarboxylic and aromatic substrates, is of great interest and is now one of the targets for enzymological analysis using site-directed mutagenesis.

From the above discussion, it is of interest to test the possibility that indole can compete with aspartate in binding to the active site of ArAT. However, neither the rate of reaction with aspartate nor the rate of reaction with tryptophan was affected by 8 mM indole (data not shown), indicating that indole has a low affinity for ArAT.

[4] Hayashi, Kagamiyama, et al., unpublished results.

Both the *erythro* and *threo* forms of 3-phenylserine were poor substrates for AspAT, although phenylalanine is a relatively good substrate. Other 3-substituted neutral amino acids, such as threonine, valine, and isoleucine, are also poor substrates for AspAT (Table I). These results show that a substituted group at the 3-position of a substrate causes unfavorable interaction of the substrate with the active site of AspAT. The only exception is 3-hydroxyaspartate. As described above, *erythro*-3-hydroxyaspartate is a slow substrate which accumulates a quinonoid intermediate, and *threo*-3-hydroxyaspartate acts as a substrate for AspAT. This indicates that when the carboxyl group of 3-hydroxyaspartate is properly fixed in the active site, the 3-hydroxy group will be oriented in such a way as to avoid unfavorable interaction with the enzyme protein. Similarly, the 3-hydroxy group of 3-phenylserine and 3-hydroxyaspartate does not cause so much unfavorable interaction with ArAT. However, threonine, valine, and isoleucine are also very poor substrates for ArAT; therefore, the orientation of the side chains of these amino acids in ArAT may be similar to that in AspAT. In summary, AspAT seems to recognize aromatic amino acids in the same manner as it recognizes other neutral amino acids, but in ArAT the mechanism of binding of aromatic amino acids is different from those of nonaromatic neutral amino acids. Nonaromatic neutral amino acids are supposed to be recognized by AspAT and ArAT through the same mechanism that the catalytic efficiency is dependent on the hydrophobicity of the side chain. Therefore, not only the binding force of aromatic substrates to the enzyme but also the mechanisms of recognition of aromatic substrates are quite different between ArAT and AspAT.

The generation of the quinonoid structure, i.e., the removal of 2-H of the amino acid substrates, has been shown to be partially rate-determining in the reaction process of AspAT (Kuramitsu et al., 1990). Experiments with [2-^{2}H]aspartate and [2-^{2}H]tryptophan demonstrated that this was also the case for the reaction of ArAT with tryptophan. This indicates that the quinonoid structure has a high energy level as compared to the other intermediates, in accordance with the fact that the quinonoid structure is present in only a small amount during the reaction of ArAT with true substrates. In the four sets of reactions of ArAT and AspAT with aspartate and tryptophan, only the reaction of tryptophan with ArAT showed a large isotope effect ($^DV = 6.0$). This may show either that in ArAT the removal of 2-H from tryptophan is a more committing step in the half-transamination reaction or that some small difference is present in the structure of the transition state to yield the quinonoid intermediate.

CONCLUSIONS

ArAT catalyzes the transamination reaction of both aromatic and dicarboxylic substrates. The active site of ArAT seems to be relatively hydrophobic compared to that of AspAT, and this may contribute to the recognition of aromatic substrates. In addition, the active site of ArAT seems to be specifically dedicated to accepting aromatic side chains. From the experiments of 3-hydroxy amino acids, the site which accepts the aromatic ring is proposed to be located in or near the carboxylate-binding region. Further insights into the structural organization of ArAT will be provided by site-directed mutagenesis and crystallographic techniques.

ACKNOWLEDGMENT

We thank Dr. Ken Hirotsu, Osaka City University, for the use of the coordinates of *E. coli* AspAT, and Dr. Sumio Tanase, Kumamoto University, for his help in drawing Figure 8.

APPENDIX

In the half-reaction of a transaminase-catalyzed reaction which is composed of multiple steps, the reaction path is expressed by the following equation:

$$E_1 \underset{k_{-1}}{\overset{k_1[S]}{\rightleftarrows}} E_2 \underset{k_{-2}}{\overset{k_2}{\rightleftarrows}} \dots E_{n-1} \underset{k_{-(n-1)}[P]}{\overset{k_{n-1}}{\rightleftarrows}} E_n \tag{1a}$$

We assume that the concentration of the product [P] is negligible and that the system reaches a microscopic steady state, which is described by the equation

$$v = k_{n-1}[E_{n-1}] = k_i[E_i] - k_{-i}[E_{i+1}] \ (i = 1 \text{ to } n-2) \tag{2a}$$

where v is the rate of the forward reaction at a given time.

Solving eq 2a, and using $[E]_T = \sum_{i=1}^{n-1} [E_i]$,

$$\frac{[E]_T}{v} = \left(\frac{1}{k_1} + \frac{k_{-1}}{k_1}\frac{1}{k_2} + \dots + \frac{k_{-1}k_{-2}\dots k_{-(n-2)}}{k_1k_2\dots k_{n-2}}\frac{1}{k_{n-1}}\right)\frac{1}{[S]} + \sum_{i=2}^{n-2}\left(\frac{1}{k_i} + \frac{k_{-i}}{k_i}\frac{1}{k_{i+1}} + \dots + \frac{k_{-i}k_{-(i+1)}\dots k_{-(n-2)}}{k_ik_{i+1}\dots k_{n-2}}\frac{1}{k_{n-1}}\right) + \frac{1}{k_{n-1}} \tag{3a}$$

From eq 3a, the $k_{cat}^{half}/K_m^{half}$ value for the forward reaction is

$$k_{cat,f}^{half}/K_{m,f}^{half} = 1/\left(\frac{1}{k_1} + \frac{k_{-1}}{k_1}\frac{1}{k_2} + \dots + \frac{k_{-1}k_{-2}\dots k_{-(n-2)}}{k_1k_2\dots k_{n-2}}\frac{1}{k_{n-1}}\right) \tag{4a}$$

Similarly, the $k_{cat}^{half}/K_m^{half}$ value for the reverse reaction is

$$k_{cat,r}^{half}/K_{m,r}^{half} = 1/\left(\frac{1}{k_{-(n-1)}} + \frac{k_{n-1}}{k_{-(n-1)}}\frac{1}{k_{-(n-2)}} + \dots + \frac{k_{n-1}k_{n-2}\dots k_2}{k_{-(n-1)}k_{-(n-2)}\dots k_{-2}}\frac{1}{k_{-1}}\right) \tag{5a}$$

From eqs 4a and 5a

$$\frac{k_{cat,f}^{half}/K_{m,f}^{half}}{k_{cat,r}^{half}/K_{m,r}^{half}} = \frac{k_1k_2\dots k_{n-1}}{k_{-1}k_{-2}\dots k_{-(n-1)}} \tag{6a}$$

The right half of eq 6a exactly expresses the equilibrium constant for the half reaction. Therefore,

$$K_{eq} = \frac{k_{cat,f}^{half}/K_{m,f}^{half}}{k_{cat,r}^{half}/K_{m,r}^{half}} \tag{7a}$$

In an overall transamination reaction depicted by the following equation,

$$E_1 \underset{k_{-1}}{\overset{k_1[A]}{\rightleftarrows}} E_2 \underset{k_{-2}}{\overset{k_2}{\rightleftarrows}} \dots E_{n-1} \underset{k_{-(n-1)}[C]}{\overset{k_{n-1}}{\rightleftarrows}} E_n \underset{k_{-n}}{\overset{k_n[B]}{\rightleftarrows}} E_{n+1} \underset{k_{-(n+1)}}{\overset{k_{n+1}}{\rightleftarrows}} \dots E_m \underset{k_{-m}[D]}{\overset{k_m}{\rightleftarrows}} E_1 \tag{8a}$$

the rate of the reaction at steady state is expressed as follows,

where the concentration of the second product, [D], is negligible

$$\frac{[E]_T}{v} = \left(\frac{1}{k_1} + \frac{k_{-1}}{k_1}\frac{1}{k_2} + \ldots + \frac{k_{-1}k_{-2}\ldots k_{-(n-1)}[C]\ldots k_{-(m-1)}}{k_1k_2\ldots k_{n-1}\ldots k_{m-1}}\frac{1}{k_m}\right)\frac{1}{[A]} + \sum_{i=2}^{n-1}\left(\frac{1}{k_i} + \frac{k_{-i}}{k_i}\frac{1}{k_{i+1}} + \ldots + \frac{k_{-i}k_{-(i+1)}\ldots k_{-(n-1)}[C]\ldots k_{-(m-1)}}{k_ik_{i+1}\ldots k_{n-1}\ldots k_{m-1}}\frac{1}{k_m}\right) + \left(\frac{1}{k_n} + \frac{k_{-n}}{k_n}\frac{1}{k_{n+1}} + \ldots + \frac{k_{-n}k_{-(n+1)}\ldots k_{-(m-1)}}{k_nk_{n+1}\ldots k_{m-1}}\frac{1}{k_m}\right)\frac{1}{[B]} + \sum_{i=n+1}^{m-1}\left(\frac{1}{k_i} + \frac{k_{-i}}{k_i}\frac{1}{k_{i+1}} + \ldots + \frac{k_{-i}\ldots k_{-(m-1)}}{k_i\ldots k_{m-1}}\frac{1}{k_m}\right) + \frac{1}{k_m} \quad (9a)$$

In the initial velocity experiments, the concentration of the first product, [C], is also negligible. Therefore,

$$\frac{[E]_T}{v} = \left(\frac{1}{k_1} + \frac{k_{-1}}{k_1}\frac{1}{k_2} + \ldots + \frac{k_{-1}k_{-2}\ldots k_{-(n-2)}}{k_1k_2\ldots k_{n-2}}\frac{1}{k_{n-1}}\right)\frac{1}{[A]} + \sum_{i=2}^{n-2}\left(\frac{1}{k_i} + \frac{k_{-i}}{k_i}\frac{1}{k_{i+1}} + \ldots + \frac{k_{-i}k_{-(i+1)}\ldots k_{-(n-2)}}{k_ik_{i+1}\ldots k_{n-2}}\frac{1}{k_{n-1}}\right) + \frac{1}{k_{n-1}} + \left(\frac{1}{k_n} + \frac{k_{-n}}{k_n}\frac{1}{k_{n+1}} + \ldots + \frac{k_{-n}k_{-(n+1)}\ldots k_{-(m-1)}}{k_nk_{n+1}\ldots k_{m-1}}\frac{1}{k_m}\right)\frac{1}{[B]} + \sum_{i=n+1}^{m-1}\left(\frac{1}{k_i} + \frac{k_{-i}}{k_i}\frac{1}{k_{i+1}} + \ldots + \frac{k_{-i}\ldots k_{-(m-1)}}{k_i\ldots k_{m-1}}\frac{1}{k_m}\right) + \frac{1}{k_m} \quad (10a)$$

By comparing eq 10a to eq 3a, the overall reaction rate is expressed using the kinetic parameters for the half-reaction

$$\frac{[E]_T}{v} = \frac{K^{half}_{m,Am}}{k^{half}_{cat,Am}}\frac{1}{[Am]} + \frac{1}{k^{half}_{cat,Am}} + \frac{K^{half}_{m,Ox}}{k^{half}_{cat,Ox}}\frac{1}{[Ox]} + \frac{1}{k^{half}_{cat,ox}} \quad (11a)$$

Rearrangement of eq 11a yields eqs 7–9.

REFERENCES

Arnone, A., Rogers, P. H., Hyde, C. C., Briley, P. D., Metzler, C. M., & Metzler, D. E. (1985) in *Transaminases* (Christen, P., & Metzler, D. E., Eds.) pp 138–154, John Wiley & Sons, New York.

Bergmann, E. D., & Bendas, H. (1950) *Comput. Rend. 231*, 361.

Fasella, P., Giartosio, A., & Hammes, G. G. (1966) *Biochemistry 5*, 197–202.

Fasella, P., & Hammes, G. G. (1967) *Biochemistry 6*, 1798–1804.

Fersht, A. (1985) *Enzyme Structure and Mechanism*, W. H. Freeman and Company, New York.

Fotheringham, I. G., Dacey, S. A., Taylor, P. P., Smith, T. J., Hunter, M. G., Finlay, M. E., Primrose, S. B., Parker, D. M., & Edwards, R. M. (1986) *Biochem. J. 234*, 593–604.

Fukui, T., Kagamiyama, H., Soda, K., & Wada, H. (1991) *Enzymes Dependent on Pyridoxal Phosphate and Other Carbonyl Compounds as Cofactors*, Pergamon Press, Oxford, UK.

Gehring, H. (1986) *Eur. J. Biochem. 159*, 291–296.

Gelfand, D. H., & Rudo, N. (1977) *J. Bacteriol. 130*, 441–444.

Gelfand, D. H., & Steinberg, R. A. (1977) *J. Bacteriol. 130*, 429–440.

Goldberg, J. M., Swanson, R. V., Goodman, H. S., & Kirsch, J. F. (1991) *Biochemistry 30*, 305–312.

Hayashi, H., Wada, H., Yoshimura, T., Esaki, N., & Soda, K. (1990) *Ann. Rev. Biochem. 59*, 87–110.

Hayashi, H., Mizuguchi, H., & Kagamiyama, H. (1993) *Biochemistry 32*, 812–818.

Inoue, K., Kuramitsu, S., Aki, K., Watanabe, Y., Takagi, T., Nishigai, M., Ikai, A., & Kagamiyama, H. (1988) *J. Biochem. 104*, 777–784.

Inoue, K., Kuramitsu, Okamoto, A., Hirotsu, K., Higuchi, T., & Kagamiyama, H. (1991) *Biochemistry 30*, 7796–7801.

Jansonius, J. N., Eichele, G., Ford, G. C., Picot, D., Thaller, C., & Vincent, M. (1985) in *Transaminases* (Christen, P., & Metzler, D. E., Eds.) pp 109–137, John Wiley & Sons, New York.

Jenkins, W. T. (1979) *Anal. Biochem. 93*, 134–138.

Jenkins, W. T., & D'Ari, L. (1966) *J. Biol. Chem. 241*, 5667–5674.

Jenkins, W. T., & Harruff (1979) *Arch. Biochem. Biophys. 192*, 421–429.

Jenkins, W. T., & Sizer, I. W. (1957) *J. Am. Chem. Soc. 79*, 2655–2656.

Johnson, G. F., Tu, J.-I., Shonka Bartlett, M. L., & Graves, D. J. (1970) *J. Biol. Chem. 245*, 5560–5568.

Kallen, R. G., Korpela, T., Martell, A. E., Matsushima, Y., Metzler, C. M., Metzler, D. E., Morozov, Yu.V., Ralston, I. M., Savin, F. A., Torchinsky, Yu.M., & Ueno, H. (1985) in *Transaminases* (Christen, P., & Metzler, D. E., Eds.) pp 37–108, John Wiley & Sons, New York.

Kamitori, S., Hirotsu, K., Higuchi, T., Kondo, K., Inoue, K., Kuramitsu, S., Kagamiyama, H., Higuchi, Y., Yasuoka, N., Kusunoki, M. H., & Matsuura, Y. (1987) *J. Biochem. 101*, 813–816.

Kamitori, S., Okamoto, A., Hirotsu, K., Higuchi, T., Kuramitsu, S., Kagamiyama, H., Matsuura, Y., & Katsube, Y. (1990) *J. Biochem. 108*, 175–184.

Kiick, D. M., & Cook, P. F. (1983) *Biochemistry 22*, 375–382.

Kiick, D. M., & Phillips, R. S. (1988) *Biochemistry 27*, 7339–7344.

Kirsch, J. F., Eichele, G., Ford, G. C., Vincent, M. G., Jansonius, J. N., Gehring, H., & Christen, P. (1984) *J. Mol. Biol. 174*, 497–525.

Kondo, K., Wakabayashi, S., & Kagamiyama, H. (1987) *J. Biol. Chem. 262*, 8648–8657.

Kuramitsu, S., Inoue, K., Ogawa, T., Ogawa, H., & Kagamiyama, H. (1985a) *Biochem. Biophys. Res. Commun. 133*, 134–139.

Kuramitsu, S., Okuno, S., Ogawa, T., Ogawa, H., & Kagamiyama, H. (1985b) *J. Biochem. 97*, 1259–1262.

Kuramitsu, S., Hiromi, K., Hayashi, H., Morino, Y., & Kagamiyama, H. (1990) *Biochemistry 29*, 5469–5476.

Malcolm, B. A., & Kirsch, J. F. (1985) *Biochem. Biophys. Res. Commun. 132*, 915–921.

Miller, S., Janin, J., Lesk, A. M., & Chothia, C. (1987) *J. Mol. Biol. 196*, 641–656.

Ovchinnikov, Yu., Egorov, C. A., Aldanova, N. A., Feigina, M. Yu., Lipkin, V. M., Abdulaev, N. G., Grishin, E. V., Kiselev, A. P., Modyanov, N. N., Braunstein, A. E., Polyanovsky, O. L., & Noskiov, V. V. (1973) *FEBS Lett. 29*, 31–34.

Powell, J. T., & Morrison, J. F. (1978) *Eur. J. Biochem. 87*, 391–400.

Rudman, D., & Meister, A. (1953) *J. Biol. Chem. 200*, 591–604.

Seville, M., Vincent, M. G., & Hahn, K. (1988) *Biochemistry 27*, 8344–8349.

Taylor, J. E., & Metzler, D. E. (1990) In *Vitamine B_6 (Ann. New York Acad. Sci. Vol 585*, Dakshinamurti, K. ed.) pp 58–67, New York Academy of Sciences, New York.

Toney, M. D., & Kirsch, J. F. (1993) *Biochemistry 32*, 1471–1479.

Velick, S. F., & Vavra, J. (1962) *J. Biol. Chem. 237*, 2109–2122.

Wada, H., & Snell, E. E. (1961) *J. Biol. Chem. 236*, 2089–2095.

Yano, T., Kuramitsu, S., Tanase, S., Morino, Y., Hiromi, K., & Kagamiyama, H. (1991) *J. Biol. Chem. 266*, 6079–6085.

Yano, T., Mizuno, T., & Kagamiyama, H. (1993) *Biochemistry 32*, 1810–1815.